European Review for Medical and Pharmacological Sciences 2020; 24: 4745-4755

TFAP2A is a novel regulator that modulates ferroptosis in gallbladder carcinoma cells *via* the Nrf2 signalling axis

H.-X. HUANG[1], G. YANG[2], Y. YANG[3], J. YAN[4], X.-Y. TANG[5], Q. PAN[5]

[1]Department of Critical Care Medicine, Children's Hospital of Chongqing Medical University, Ministry of Education Key Laboratory of Child Development and Disorders, China International Science and Technology Cooperation Base of Child Development and Critical Disorders, Chongqing, P.R. China
[2]Department of Urology Surgery, The First Affiliated Hospital of Chongqing Medical University, Chongqing, P.R. China
[3]Department of Neurosurgery, West China Hospital, Sichuan University, Chengdu, P.R. China
[4]Chongqing Key Laboratory of Translational Research for Cancer Metastasis and Individualized Treatment, Chongqing University Cancer Hospital, Chongqing, P.R. China
[5]Department of Dermatology, Chongqing Traditional Chinese Medicine Hospital, Chongqing, P.R. China

Haixia Huang, Guang Yang, Yuan Yang and *Jin Yan* contributed equally to this work

Abstract. – OBJECTIVE: Ferroptosis is a recently identified form of controlled cell death generally associated with the accumulation of lipid-associated reactive oxygen species (ROS). However, the molecular mechanisms underlying ferroptosis have not been established.

MATERIALS AND METHODS: Microarray expression data for three human gallbladder carcinoma (GBC) and matched non-tumour specimens were downloaded from the Gene Expression Omnibus (GEO) repository. Candidate genes were filtered using bioinformatic analysis. After cell transfection, candidate gene impacts on cell proliferation, migration, invasion and ferroptosis (ferrous iron (Fe^{2+}) and malondialdehyde (MDA) levels) were assessed.

RESULTS: We screened 626 differentially expressed genes (DEGs) including 465 that were downregulated and 161 that were upregulated in the three tissue pairs. These DEGs were used to construct a protein-protein interaction (PPI) network. Functional enrichment analysis revealed the top three modules in the network and four hub genes. Transcription factor AP-2 alpha (TFAP2A) was screened and showed overexpression in The Cancer Genome Atlas (TCGA) digestive system tumour data and a relationship with clinical survival. *In vitro*, GBC exhibited upregulated expression of TFAP2A, whose inhibition reduced GBC cell proliferation, migration, and invasion. Fe^{2+} and MDA levels were elevated. Moreover, Kyoto Encyclopedia of Genes and Genomes (KEGG) pathway analysis revealed TFAP2A enrichment in oxidative stress. Subsequent experiments demonstrated that TFAP2A silencing attenuated the expression of key genes associated with oxidative stress such as heme oxygenase 1 (HO-1), nuclear factor erythroid 2 like 2 (Nrf2), ferritin heavy chain 1 (FTH1) and NAD(P)H quinone dehydrogenase 1 (NQO1).

CONCLUSIONS: Bioinformatic and experimental analyses reveal that TFAP2A plays a vital role in ferroptosis and hence is a potential therapeutic target for GBC treatment.

Key Words:
Gallbladder carcinoma, TFAP2A, Ferroptosis, Oxidative stress.

Introduction

Gallbladder carcinoma (GBC) is a common malignancy of the digestive tract[1]. Over the years, the GBC incidence in China has steadily increased[2]. Obesity, cholelithiasis, and chronic cholecystitis are some of the important risk factors for GBC[3,4]. Surgical resection is considered to be the most effective treatment for GBC. However, due to the lack of an effective early diagnostic method, diagnosis occurs at an advanced stage, and the majority of GBC cases are incidentally

Corresponding Author: Qi Pan, MD; e-mail: qi_pan@vip.sina.com

discovered following laparoscopic cholecystectomy. Late diagnosis combined with the anatomical structure of the gallbladder results in a poor prognosis[3]. Therefore, sensitive and specific biomarkers for use in the diagnosis and prognosis of GBC are urgently needed to develop novel therapeutic strategies[5].

Microarray technology has recently been used as a promising diagnostic and prognostic tool in medical oncology due to its wide application in molecular diagnosis and cancer classification, identification of new drug targets, and prediction of tumour response[6-8]. Multiple studies[9,10] have identified a number of differentially expressed genes (DEGs) in many cancer types through microarray analysis. Compared with Sanger sequencing of cDNA libraries, microarrays are relatively easy to perform and inexpensive. Bioinformatic analysis and microarray technology for mRNA are often utilized to identify DEGs in GBC. Using DNA microarray technology, Chen et al[11] determined that Beclin-1 plays an important role in GBC development. Therefore, crucial genes and key pathways in GBC can be identified with bioinformatic analysis and microarray technology.

Ferroptosis is an iron-dependent, oxidative, non-apoptotic form of cell death that is different from necrosis, apoptosis, and autophagy in terms of cell morphology and function[12]. It is characterized by the build-up of lipid reactive oxygen species (ROS)[13]. Ferroptosis induction has been reported to promote selective killing of multiple types of tumour cells; hence, it is a promising strategy for cancer therapy[14,15]. Recently, key ferroptosis regulators have been identified in defined tumour cell populations. The Nrf2 gene and its targets are involved in the oxidative stress response and play a regulatory role in ferroptosis[16]. Glutathione peroxidase-4 (GPX4), a novel member of the selenium-dependent glutathione peroxidases in mammals, is reported to suppress lipid ROS accumulation during ferroptotic tumour cell death[17]. However, the principal regulator and signalling pathways of ferroptosis have not been established. In this study, microarray technology was employed to obtain gene expression profiles, while bioinformatic analysis was used to investigate DEGs to identify key biomarkers in GBC. The study revealed that TFAP2A was associated with the malignant phenotypes of GBC cells and ferroptosis. Furthermore, we examined the molecular mechanism utilizing TFAP2A inhibition.

Materials and Methods

Microarray Data

The microarray expression profile dataset GSE74048 was downloaded from the Gene Expression Omnibus (GEO) database (http://www.ncbi.nlm.nih.gov/geo/). This dataset contained six samples, three GBC samples and three matched non-tumour samples. Gene expression was evaluated using an Agilent GPL20115 platform (Agilent-067406 Human Genome Microarray, Santa Clara, CA, USA).

DEG Identification

The raw data of GSE74048 in TXT files were processed using GeneSpring software (version 14.8, Agilent, Santa Clara, CA, USA). Hierarchical clustering analysis was employed to subcategorize the dataset into two groups based on shared similarities and the expression pattern in the GBC and matched non-tumour samples. Principal component analysis (PCA) was utilized to assess the probe quality control in GeneSpring. We then removed probes with intensity values not exceeding the 20th percentile using the "filter ProbeSets by Expression" option. The DEGs were compared using a *t*-test with a fold change (FC) > 2 and a *p*-value <0.05 as the cut-offs for statistical significance.

Functional Enrichment Analysis of DEGs

The Database for Annotation, Visualization and Integrated Discovery (DAVID; https://david.ncifcrf.gov/) was used for functional annotation clustering[18] of all up- or downregulated genes identified with the three GBC and matched non-tumour samples with a false discovery rate (FDR) <0.05. Kyoto Encyclopedia of Genes and Genomes (KEGG) pathway[19] and Gene Ontology (GO)[20] analyses were then performed.

ClusterOne is used to identify potentially overlapping protein complexes in protein-protein interaction (PPI) networks[21]. The DEGs were mapped with ClusterOne to examine the interactions among the DEGs, and a sweep for the 'd' (minimum cluster density) and 's' (minimum size) parameters in ClusterOne was performed. The default parameters used were s=4 and d=0.1.

Cell Culture

Immortalized non-tumourigenic human intrahepatic bile duct cells (H69) and gallbladder cancer cells (GBC-SD) were obtained from the Chinese Academy of Sciences cell bank. These cells were

grown in Roswell Park Memorial Institute-1640 (RPMI-1640) medium (Invitrogen, Carlsbad, CA, USA) supplemented with 10% foetal bovine serum (FBS; Invitrogen, Carlsbad, CA, USA) and 1% streptomycin/penicillin at 37°C and 5% CO_2.

RNA Isolation and Quantitative Real Time-Polymerase Chain Reaction (qRT-PCR) Assay

RNAiso Plus (TaKaRa, Beijing, China) was used to isolate total cellular RNA according to the kit protocol. Then, the isolated RNA was converted into cDNA using the PrimeScriptTM RT Reagent Kit with gDNA Eraser (TaKaRa, Beijing, China). SYBR Premix Ex Taq II (TaKaRa, Beijing, China) reagent was utilized for qRT-PCR. The following primer sequences were used: β-actin (F: 5'-CCA CGA AAC TAC CTT CAA CTC C-3'; R: 5'-GTG ATC TCC TTC TGC ATC CTG T-3'); *Nrf2* (F: 5'-TCA GCG ACG GAA AGA GTA TGA-3'; R: 5'-CCA CTG GTT TCT GAC TGG ATG T-3'); and *TFAP2A* (F: 5'-CGA TGC GGC AGG AAC ACT GGA GGT AGA TT-3'; R: 5'-TGC TGG TGG TAG TGC TTG CTC AGT CGT T-3'). qRT-PCR results were assessed using the $2^{-\Delta\Delta CT}$ method, and the expression of β-actin was used as the reference. This experiment was run in triplicate.

Cell Transfection

A total of three TFAP2A-siRNAs used for TFAP2A silencing and a negative control (si-NC) were obtained from RiboBio (Guangzhou, Guangdong, China). The following sequences were used: si-TFAP2A #1 (sense: 5'-GAG GAA GAT CTT TAA GAG A-3'); si-TFAP2A #2 (sense: 5'-CAC GGA CAA CAA CGC CAA A-3'); si-TFAP2A #3 (sense: 5'-GTC TCC GCC ATC CCT ATT A-3'). We plated cells (10^5 cells/well) in 6-well plates and grew them to 70-80% confluence. Cells were prepared for transient transfection with siRNA/NC (100 nM) using Lipofectamine 2000 (Invitrogen, Carlsbad, CA, USA) and monitored for 48 hours. These cells were utilized to conduct further experimental tests.

Cell Proliferation

Prepared cells (4×10^3 cells/well) were seeded in 96-well plates and incubated for 0, 24, 48, or 72 hours. Afterwards, we added Cell Counting Kit-8 (CCK8) reagent (Dojindo Molecular Technologies, Kumamoto, Japan) to the cells and incubated them in the dark for 90 minutes. Cell viability was assessed with a standard curve for absorbance at 450 nm.

Wound-Healing Assay

The migratory potential of GBC-SD cells was determined with a wound-healing assay. Cells were seeded in 96-well plates and grown to 100% confluence. Next, a sterile pipette tip was utilized to create a scratch wound in the cell monolayer. We then performed phosphate-buffered saline (PBS) washing to remove detached cells. Cell images were acquired imaged at 0 hours and after 24 hours of incubation in serum-free medium.

Cell Migration/Invasion Assays

Transwell chamber assays were employed to evaluate the invasion and migration of GBC-SD cells. Briefly, untreated and treated GBC-SD cells were suspended in FBS-free medium. One hundred microliters of cell suspension were removed from the upper chamber, and 600 μL of complete medium was added to the lower chamber. To assess invasion, Matrigel (BD Biosciences, Franklin Lakes, NJ, USA) was used to coat the upper chamber prior to cell inoculation. In the upper chambers, we added 4×10^4 cells and allowed them to incubate for 24 hours. Then, the cells were fixed in 4% paraformaldehyde for 15 minutes and stained with a 0.1% crystal violet solution for 10 minutes prior to removal of the inner layer. The plates were imaged with a microscope. For each group, we estimated the number of cells in 3 randomly chosen microscopic fields.

Western Blot Analysis

Western blotting was performed with isolated cellular proteins. First, a bicinchoninic acid (BCA) protein assay kit (Beyotime, Shanghai, China) was utilized to quantify protein concentrations in samples. Subsequently, the protein samples were resolved by sodium dodecyl sulfate polyacrylamide gel electrophoresis (SDS-PAGE) on 10% gels and electrotransferred to polyvinylidene difluoride (PVDF) membranes. The membranes were blocked in 5% fat-free milk for 10 minutes and incubated overnight at 4°C with the appropriate primary antibodies. The membranes were rinsed three times with Tris-Buffered Saline and Tween-20 (TBST) and then incubated with secondary antibodies at room temperature for 1 hour. Next, we used a TBST solution to wash the membranes twice. Visualization of the immunoblotted bands was performed using an enhanced chemiluminescence (ECL) solution (Wanleibio, Shenyang, China) in the dark.

Iron Assay

The relative iron concentration in cell lysates was determined using an iron assay kit (BioAssay Systems, Hayward, CA, USA) following the manufacturer's instructions.

Lipid Peroxidation Assay

The Lipid Peroxidation (MDA) Assay Kit (Nanjing Jiancheng Bioengineering Institute, Nanjing, China) was used to determine the malondialdehyde (MDA) concentration in cell lysates following the manufacturer's instructions.

Statistical Analysis

GraphPad Prism analysis software was utilized to perform statistical analyses. Data are presented as the mean ± standard deviation (SD). Means of different groups were compared with Student's *t*-test, whereas mean values of more than two groups were compared using one-way ANOVA, followed by post-hoc test with Bonferroni's methods. A p-value < 0.05 was considered statistically significant.

Results

Identification of DEGs

DEGs were defined as genes meeting the cut-offs of $p < 0.05$ and FC > 2.0. Overall, 626 DEGs were identified, of which 465 were downregulated and 161 were upregulated. Figure 1A shows the DEG expression heat map.

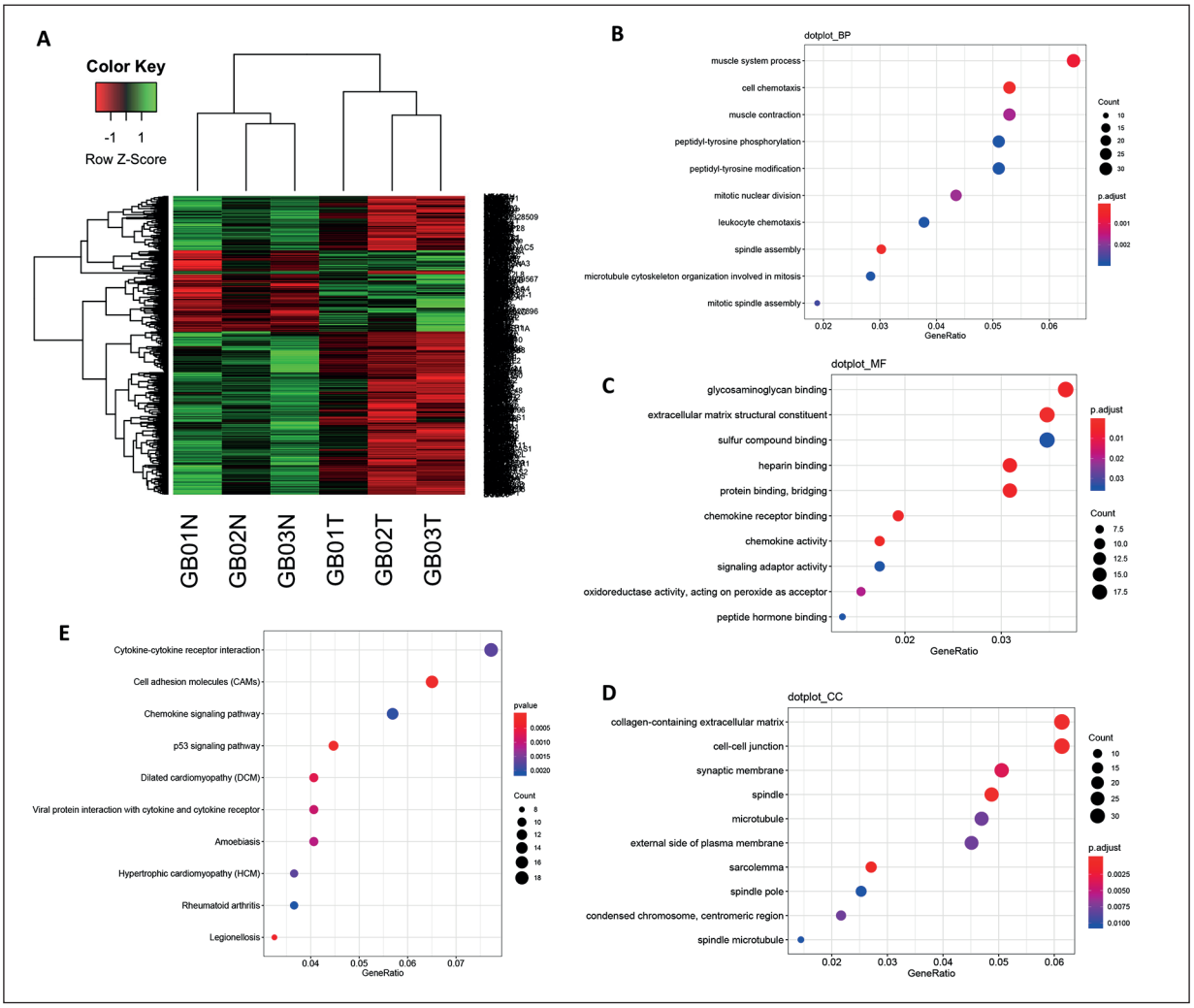

Figure 1. DEG identification and functional enrichment. **A**, The distributions of up- and downregulated DEGs between three GBC and matched non-tumour tissue samples (fold change > 1 and FDR < 0.05). The rows represent the genes, while the columns represent the samples. Red denotes genes that were suppressed in GBC; green denotes upregulated genes. **B-D**, Top 10 biological process, molecular function, and cellular component terms. **E**, Top enriched KEGG pathways.

Enrichment Analysis of DEGs

Based on GO analysis, the DEGs were functionally enriched in biological processes (BP) related to a muscle system process, cell chemotaxis and spindle assembly (Figure 1B). DEGs were also highly enriched in molecular functions (MF), such as an extracellular matrix structural constituent, glycosaminoglycan binding, and protein binding (Figure 1C). Additionally, for cellular components (CC), DEGs were enriched in the collagen-containing extracellular matrix, cell-cell junctions, and sarcolemma (Figure 1D).

KEGG pathway analysis showed that the 626 DEGs were highly enriched in 'cell adhesion molecules (CAMs)', 'cytokine-cytokine receptor interaction', and the 'p53 signalling pathway' (Figure 1E).

The top 19 signalling pathways in the interaction network are shown in Figure 2A. The results showed that oxidative stress could interact between the PI3K-Akt and Rap1 pathways. Additionally, a more complex subnetwork contained chemokines, cytokine-cytokine receptor interactions, NF-kappa B, amoebiasis, rheumatoid arthritis, and legionellosis. Figure 2B shows that TFAP2A was enriched in oxidative stress; BCL2, CDK1, SFN, RRM2, SESN3, and SESN1 were enriched in the p53 signalling pathway; and SORBS1, CYP4A11, CYP27A1, ADIPOQ, LPL, and RXRG were enriched in the PPAR signalling pathway.

PPI Network of DEGs

A PPI network for the 626 DEGs created using ClusterOne identified the interactions between genes at the protein level. The top three significant modules were selected (Figure 2C) based on the High-quality INTeractomes (HINT) database. Four DEGs including three upregulated genes (PLK1, SFN, and TFAP2A) and one downregulated gene (RUNX1T1) were identified. TFAP2A exhibited the most signif-

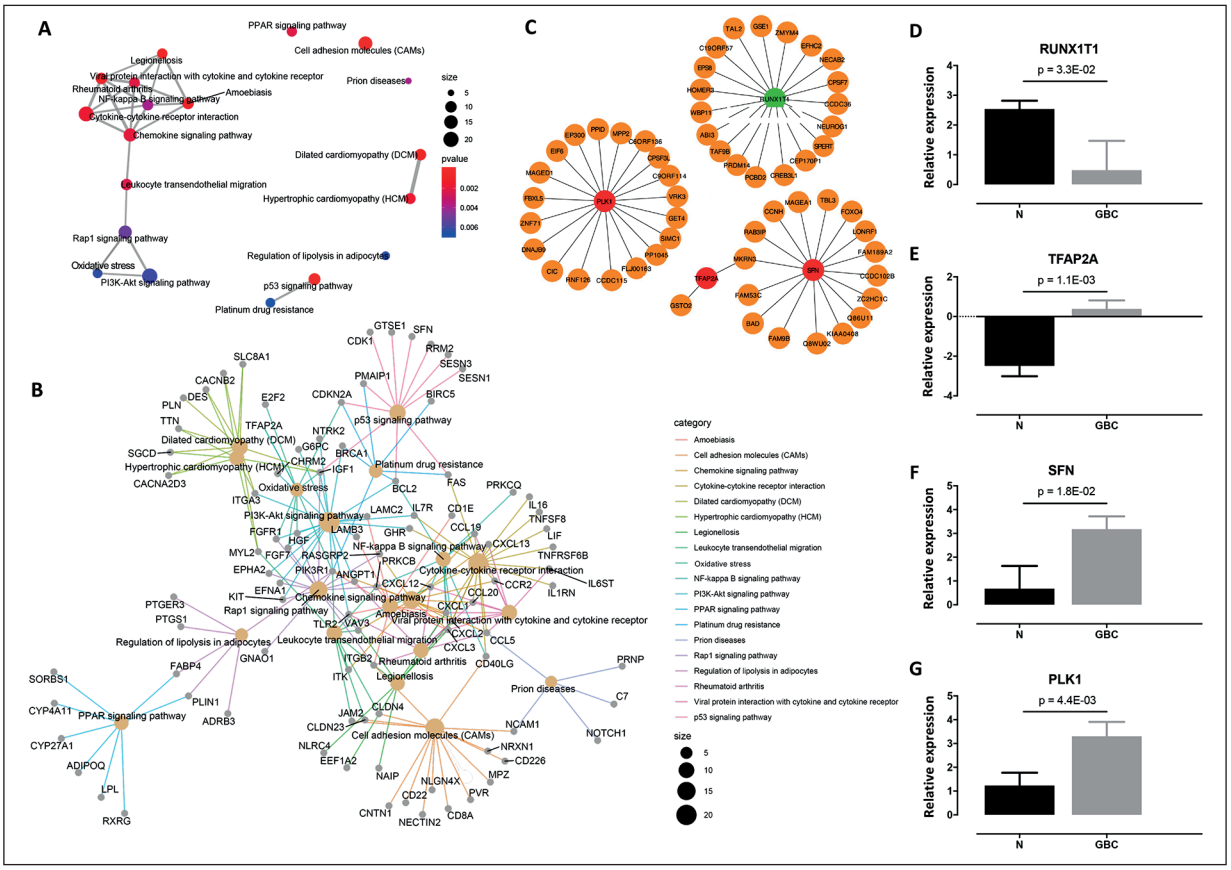

Figure 2. Identification of hub genes. **A**, DEG-enriched interaction network. **B**, Interaction network for DEGs and pathways. **C**, Top three modules in the protein-protein interaction network. Red denotes overexpressed DEGs; green denotes suppressed DEGs. **D-G**, Levels of hub genes in GBC microarray expression profiles.

icant differential expression between the three non-tumour and GBC samples (p=1.1E-03) (Figure 2D-G), indicating that it plays a critical role in GBC.

TFAP2A Knockdown Inhibits GBC Cell Proliferation

To explore the relationship between TFAP2A and clinical implications, we validated TFAP2A expression and associations with survival with The Cancer Genome Atlas (TCGA) data. Although GBC is not included in the TCGA, TFAP2A was overexpressed in digestive system tumours, and upregulated TFAP2A expression was associated with poor survival in TCGA liver cancer (LIHC), stomach adenocarcinoma (STAD) and pancreatic adenocarcinoma (PAAD) datasets (Figure 3A-D). *In vitro*, TFAP2A expression was remarkably upregulated in GBC-SD cell lines (Figure 3E-F). In addition, TFAP2A mRNA and protein levels were markedly lower in GBC-SD cells transfected with si-TFAP2A #1, si-TFAP2A #2 or si-TFAP2A #3 than in GBC-SD cells in the si-NC and control groups (Figure 3G-H). This indicated successful TUG1 knockout, and si-TFAP2A #1 was used for subsequent experiments. A CCK8 assay revealed that the GBC-SD cell proliferation rate was considerably lower in the TFAP2A siRNA group than in the NC siRNA group (Figure 3I).

TFAP2A Knockdown Represses GBC Cell Invasion and Migration

The migration of GBC cells was assessed using a wound-healing assay. There were significant reductions in invasive and migratory

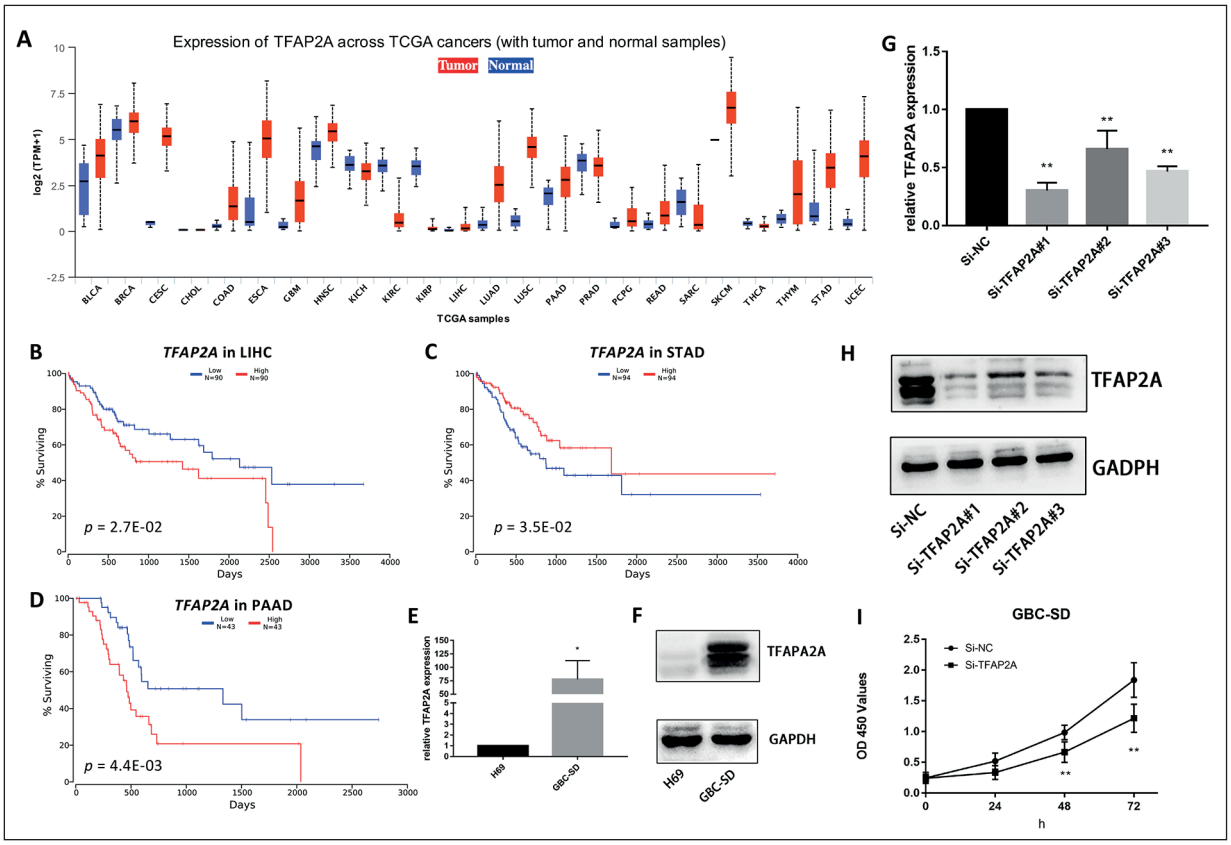

Figure 3. TFAP2A expression. **A**, TFAP2A mRNA expression in TCGA pan-cancer datasets. **B-D**, Clinical implications of differential TFAP2A expression in TCGA liver cancer (LIHC, n=360), stomach adenocarcinoma (STAD, n=376) and pancreatic adenocarcinoma (PAAD, n=172). **E-F**, qRT-PCR and Western blot analyses showing TFAP2A expression levels in a GBC cell line. **G-H**, Expression levels of TFAP2A in GBC-SD cells after transfection with siRNAs against TFAP2A or si-NC as determined by qRT-PCR and Western blotting. **I**, Cell viability of GBC-SD cells transfected with Si-NC or Si-TFAP2A as assessed by CCK-8 assays. The tests were carried out in triplicate. Data are presented as the mean ± SD (**: Si-NC *vs.* Si-TFAP2A, ***p*<0.01).

abilities in TFAP2A-knockdown cells compared with NC-siRNA-transfected cells (Figure 4A and B). These findings were consistent with those of the wound-healing assay. These findings suggest that TFAP2A may function in GBC cell metastasis.

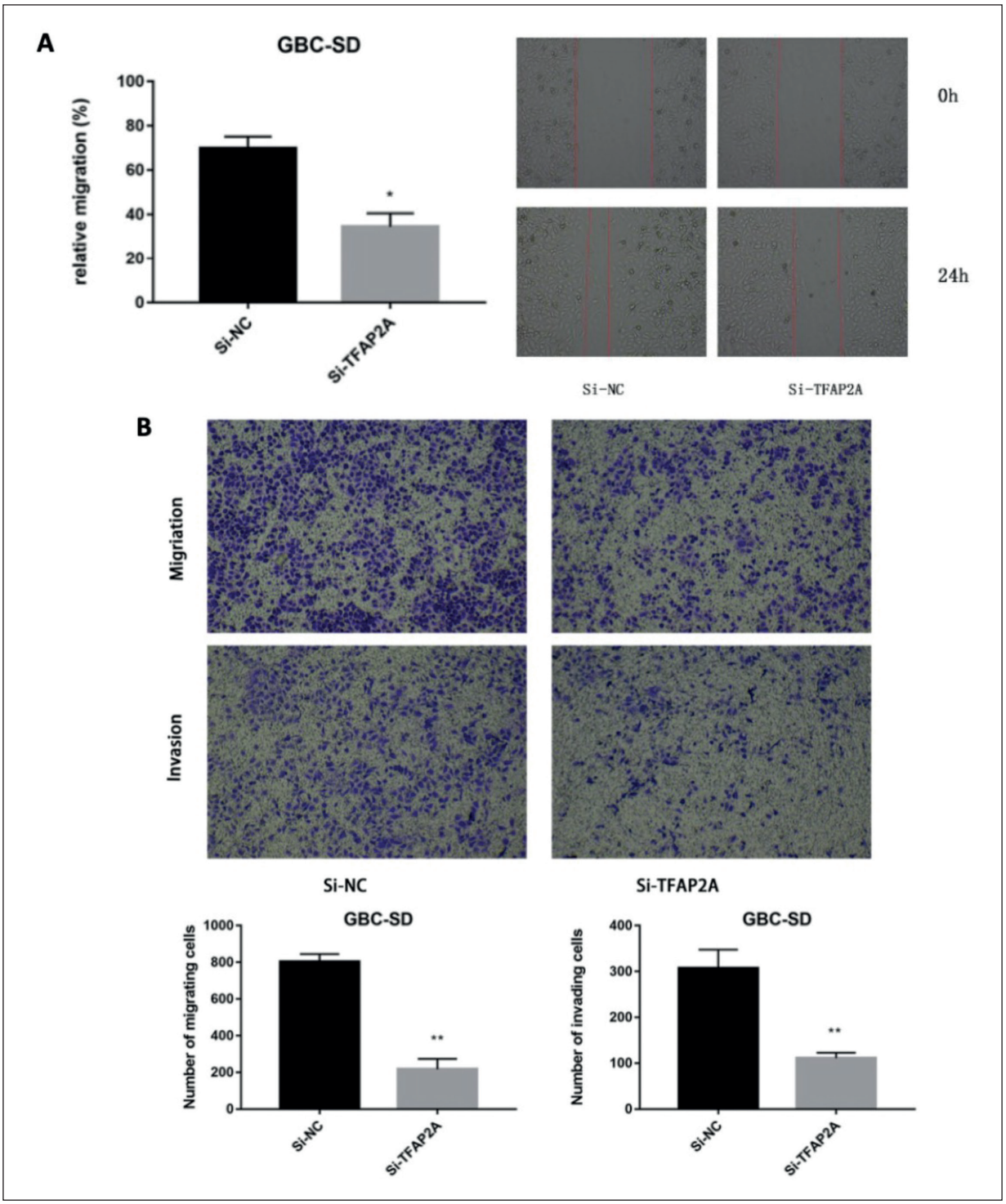

Figure 4. Migration and invasion assays. **A**, Evaluation of wound-healing ability (magnification 100×). **B**, The invasive and migratory capacities of GBC-SD cells in various treatments as assessed by a transwell migration/invasion assay. All assays were carried out in triplicate. Data are presented as the mean ± SD (*: Si-NC *vs.* Si-TFAP2A, **p<0.01, *p<0.05).

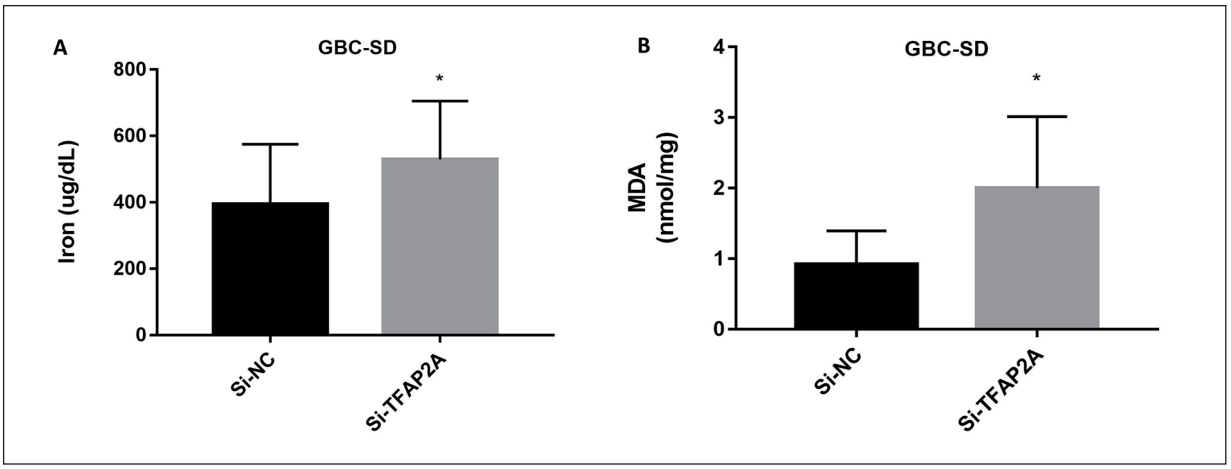

Figure 5. TFAP2A-mediated regulation of ferroptosis. **A-B**, Fe^{2+} and MDA levels assayed after TFAP2A silencing.

TFAP2A Inhibition Promotes Ferroptosis

The two major features of ferroptosis are iron dependency and lipid peroxide accumulation. Therefore, since ferrous iron (Fe^{2+}) is a critical factor in ferroptosis, the effect of TFAP2A on the Fe^{2+} level was determined. TFAP2A knockdown increased intracellular Fe^{2+} levels (Figure 5A). In addition, MDA is one of the most important lipid peroxidation by-products; hence, we assessed whether TFAP2A regulates MDA accumulation in GBC cells. Figure 5B shows that TFAP2A inhibition increased MDA accumulation in GBC-SD cells. These findings suggest that TFAP2A inhibition promotes ferroptosis in GBC cells.

TFAP2A Silencing Suppresses the Nrf2 Pathway

As shown in Figure 6A, TFAP2A was enriched in oxidative stress. Subsequently, the relationships between TFAP2A and several typical oxidative stress genes (Nrf2, HO-1, NQO1, and FTH1) identified with the GBC microarray data were examined (Figure 6B). TFAP2A was found to be positively correlated with Nrf2, HO-1 and FTH1. The GBC microarray data highlighted the expression of TFAP2A and Nrf2 pathway members (Figure 6C).

The Nrf2 gene was overexpressed in the GBC-SD cell line at both the mRNA and protein levels, which was consistent with the GBC

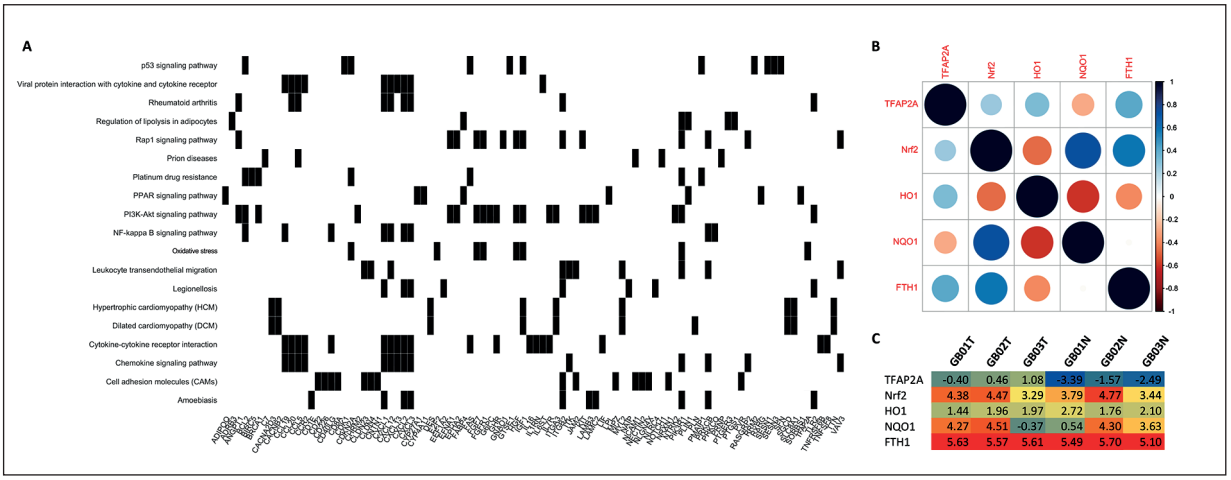

Figure 6. Functional enrichment related to TFAP2A. **A**, Signalling pathways and a heat map showing the relationships between signalling pathways and related genes. **B**, Correlation between TFAP2A and the Nrf2 oxidative stress pathway. **C**, Heat map showing the expression of TFAP2A and Nrf2 pathway genes in GBC microarray data.

expression profile findings (Figure 7A and B). TFAP2A knockdown decreased the expression of Nrf2, HO-1, NQO1 and FTH1 (Figure 7C and D). These findings indicate that TFAP2A may regulate ferroptosis through the Nrf2 pathway.

Discussion

GBC ranks fifth among the most prevalent digestive tract cancers[1]. Despite extensive research on the relationship between abnormal expression of oncogenes and tumorigenesis, the potential molecular mechanism of GBC remains largely unclear. Therefore, the current study employed bioinformatic analysis and microarray tools to reveal the molecular mechanisms underlying GBC.

A total of 626 DEGs were identified and found to be involved in cell chemotaxis, spindle assembly, and glycosaminoglycan binding. Recent studies have reported an evident difference in cell chemotaxis between the diffuse and intestinal types of gastric cancer[22]. Disruption of spindle assembly induces cancer cell apoptosis[23], while inhibition of tumour microenvironment glycosaminoglycans enhances tumour cell metastatic potential[24].

This study is the first to report TFAP2A overexpression and its role as a candidate marker in the regulation of malignant phenotypes and ferroptosis in GBC. TFAP2A is a transcription factor, and its abnormal expression is closely associated with progression in many malignant tumours[25,26]. TFAP2A expression is reported to be upregulated in hepatocellular carcinoma and glioma[27,28]. In this study, TFAP2A expression was upregulated in GBC-SD cells relative to a human intrahepatic bile duct cell line. These findings are consistent with those reported in previous researches. Studies continue to demonstrate that TFAP2A plays regulatory roles in cell biological behaviours, such as cell proliferation, migration, invasion, and differentiation[29-31]. Schulte et al[32] reported that TFAP2A overexpression is associated with cell differentiation and proliferation in neuroblastoma. In this study, we demonstrate that TFAP2A inhibition decreases GBC cell proliferation, migration, invasion and ferroptosis. Numerous ferroptosis regulators have been reported in several tumours[33,34]; however, this

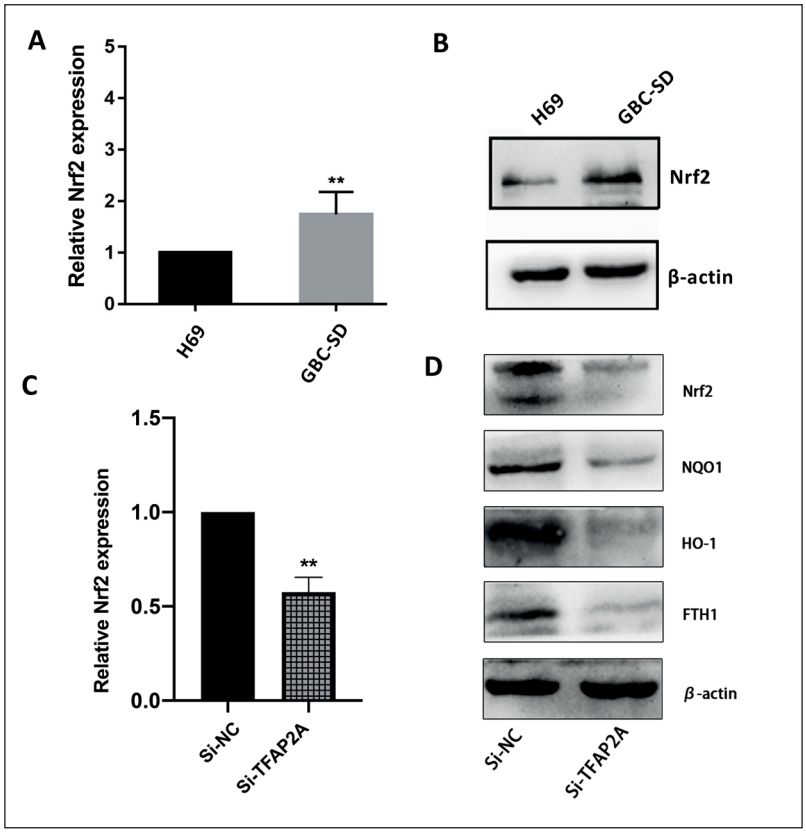

Figure 7. TFAP2A modulates the Nrf2 pathway. **A-B**, Western blot and qRT-PCR assays showing Nrf2 expression in a GBC cell line. **C**, Nrf2 expression as measured by qRT-PCR. **D**, Expression of Nrf2 and its targets determined by Western blot analysis.

is the first report indicating that TFAP2A functions as a ferroptosis regulator in GBC.

Nrf2 prevents damage caused by oxidative stress. Indeed, activated Nrf2 promotes cancer development and progression[35]. Furthermore, abnormal expression of genes associated with the Nrf2 pathway is often detected in various malignancies, suggesting the involvement of this pathway in tumour metastasis[36,37]. Compelling evidence suggests that ferroptosis is regulated by the Nrf2 pathway. Sun et al[33] reported that stimulation of the Nrf2 pathway protected against ferroptosis in hepatocellular carcinoma. Shin et al[38] indicated that Nrf2 knockdown sensitized GPX4 inhibitor-induced ferroptosis in head and neck cancer. Our findings revealed that TFAP2A was enriched in oxidative stress and that TFAP2A knockdown suppressed the expression of Nrf2 and its targets.

Conclusions

In summary, using bioinformatic analysis and microarray technology, TFAP2A was identified as a candidate marker for GBC from 626 DEGs. In addition, TFAP2A silencing suppressed invasion, proliferation, and migration and induced ferroptosis by inactivating the Nrf2 pathway in GBC cells. Therefore, this study describes the regulatory mechanism involving TFAP2A in GBC, which is also a potential therapeutic target for GBC treatment.

Conflict of Interest

The Authors declare that they have no conflict of interests.

Funding

This work was sponsored by the China Postdoctoral Science Foundation (2019M653831XB to Q.P.), Natural Science Foundation of Chongqing, China (cstc2019jcyj-msxmX0095 to Q.P.), National Natural Science Young Foundation of China (81904218 to Q.P. and 81902532 to Y.Y.) and Spark Project of Sichuan University (2082604401223 to Y.Y.).

Authors' Contribution

Q.P. conceived and designed the study. H.X.H., G.Y., J.Y. and Q.P. performed the majority of the experiments and wrote the paper. All authors approved the manuscript and agree to be accountable for all aspects of the research to ensure that issues related to the accuracy or integrity of any part of the work are appropriately investigated and resolved.

References

1) Baldvinsdottir B, Hauksson H, Haraldsdottir KH. Gallbladder carcinoma in Iceland 2004-2013. Laeknabladid 2017; 103: 179-183.
2) Hsing AW, Gao YT, Han TQ, Rashid A, Sakoda LC, Wang BS, Shen MC, Zhang BH, Niwa S, Chen J, Fraumeni JF, Jr. Gallstones and the risk of biliary tract cancer: a population-based study in China. Br J Cancer 2007; 97: 1577-1582.
3) Boutros C, Gary M, Baldwin K, Somasundar P. Gallbladder cancer: past, present and an uncertain future. Surg Oncol 2012; 21: e183-e191.
4) Stinton LM, Shaffer EA. Epidemiology of gallbladder disease: cholelithiasis and cancer. Gut Liver 2012; 6: 172-187.
5) Srivastava K, Srivastava A, Mittal B. Potential biomarkers in gallbladder cancer: present status and future directions. Biomarkers 2013; 18: 1-9.
6) Kulasingam V, Diamandis EP. Strategies for discovering novel cancer biomarkers through utilization of emerging technologies. Nat Clin Pract Oncol 2008; 5: 588-599.
7) Nannini M, Pantaleo MA, Maleddu A, Astolfi A, Formica S, Biasco G. Gene expression profiling in colorectal cancer using microarray technologies: results and perspectives. Cancer Treat Rev 2009; 35: 201-209.
8) Bustin SA, Dorudi S. Gene expression profiling for molecular staging and prognosis prediction in colorectal cancer. Expert Rev Mol Diagn 2004; 4: 599-607.
9) Chen H, Fan Y, Xu W, Chen J, Meng Y, Fang D, Wang J. Exploration of miR-1202 and miR-196a in human endometrial cancer based on high throughout gene screening analysis. Oncol Rep 2017; 37: 3493-3501.
10) Shen LI, Liu L, Yang Z, Jiang N. Identification of genes and signaling pathways associated with squamous cell carcinoma by bioinformatics analysis. Oncol Lett 2016; 11: 1382-1390.
11) Chen Y, Yan J, Yu S, Wang X, Zheng Q. Over-expression of beclin-1 in gallbladder carcinoma and its relationship with prognosis. Contemp Oncol (Pozn) 2014; 18: 171-176.
12) Dixon SJ, Lemberg KM, Lamprecht MR, Skouta R, Zaitsev EM, Gleason CE, Patel DN, Bauer AJ, Cantley AM, Yang WS, Morrison B, 3rd, Stockwell BR. Ferroptosis: an iron-dependent form of nonapoptotic cell death. Cell 2012; 149: 1060-1072.
13) Yagoda N, von Rechenberg M, Zaganjor E, Bauer AJ, Yang WS, Fridman DJ, Wolpaw AJ, Smukste I, Peltier JM, Boniface JJ, Smith R, Lessnick SL, Sahasrabudhe S, Stockwell BR. RAS-RAF-MEK-dependent oxidative cell death involving voltage-dependent anion channels. Nature 2007; 447: 864-868.
14) Yu Y, Xie Y, Cao L, Yang L, Yang M, Lotze MT, Zeh HJ, Kang R, Tang D. The ferroptosis inducer erastin enhances sensitivity of acute myeloid leukemia cells to chemotherapeutic agents. Mol Cell Oncol 2015; 2: e1054549.

15) Jiang L, Kon N, Li T, Wang SJ, Su T, Hibshoosh H, Baer R, Gu W. Ferroptosis as a p53-mediated activity during tumour suppression. Nature 2015; 520: 57-62.

16) Abdalkader M, Lampinen R, Kanninen KM, Malm TM, Liddell JR. Targeting Nrf2 to suppress ferroptosis and mitochondrial dysfunction in neurodegeneration. Front Neurosci 2018; 12: 466.

17) Imai H, Matsuoka M, Kumagai T, Sakamoto T, Koumura T. Lipid peroxidation-dependent cell death regulated by GPx4 and ferroptosis. Curr Top Microbiol Immunol 2017; 403: 143-170.

18) Dennis G, Sherman BT, Hosack DA, Yang J, Gao W, Lane HC, Lempicki RA. DAVID: database for annotation, visualization, and integrated discovery. Genome Biol 2003; 4: R60.

19) Ogata H, Goto S, Sato K, Fujibuchi W, Bono H, Kanehisa M. KEGG: Kyoto Encyclopedia of Genes and Genomes. Nucleic Acids Res 1999; 27: 29-34.

20) Ashburner M, Ball CA, Blake JA, Botstein D, Butler H, Cherry JM, Davis AP, Dolinski K, Dwight SS, Eppig JT, Harris MA, Hill DP, Issel-Tarver L, Kasarskis A, Lewis S, Matese JC, Richardson JE, Ringwald M, Rubin GM, Sherlock G. Gene ontology: tool for the unification of biology. The gene ontology consortium. Nat Genet 2000; 25: 25-29.

21) Nepusz T, Yu H, Paccanaro A. Detecting overlapping protein complexes in protein-protein interaction networks. Nat Methods 2012; 9: 471-472.

22) Perrot-Applanat M, Vacher S, Pimpie C, Chemlali W, Derieux S, Pocard M, Bieche I. Differential gene expression in growth factors, epithelial mesenchymal transition and chemotaxis in the diffuse type compared with the intestinal type of gastric cancer. Oncol Lett 2019; 18: 674-686.

23) Bond MJ, Bleiler M, Harrison LE, Scocchera EW, Nakanishi M, G-Dayanan N, Keshipeddy S, Rosenberg DW, Wright DL, Giardina C. Spindle assembly disruption and cancer cell apoptosis with a CLTC-binding compound. Mol Cancer Res 2018; 16: 1361-1372.

24) Pereira JX, Dos Santos SN, Pereira TC, Cabanel M, Chammas R, de Oliveira FL, Bernardes ES, El-Cheikh MC. Galectin-3 regulates the expression of tumor glycosaminoglycans and increases the metastatic potential of breast cancer. J Oncol 2019; 2019: 9827147.

25) Lian W, Zhang L, Yang L, Chen W. AP-2α reverses vincristine-induced multidrug resistance of SGC7901 gastric cancer cells by inhibiting the Notch pathway. Apoptosis 2017; 22: 933-941.

26) Hallberg AR, Vorrink SU, Hudachek DR, Cramer-Morales K, Milhem MM, Cornell RA, Domann FE. Aberrant CpG methylation of the TFAP2A gene constitutes a mechanism for loss of TFAP2A expression in human metastatic melanoma. Epigenetics 2014; 9: 1641-1647.

27) Su W, Xia J, Chen X, Xu M, Nie L, Chen N, Gong J, Li X, Zhou Q. Ectopic expression of AP-2α transcription factor suppresses glioma progression. Int J Clin Exp Pathol 2014; 7: 8666-8674.

28) Huang W, Chen C, Liang Z, Qiu J, Li X, Hu X, Xiang S, Ding X, Zhang J. AP-2alpha inhibits hepatocellular carcinoma cell growth and migration. Int J Oncol 2016; 48: 1125-1134.

29) Lin X, Yang H, Wang L, Li W, Diao S, Du J, Wang S, Dong R, Li J, Fan Z. AP2a enhanced the osteogenic differentiation of mesenchymal stem cells by inhibiting the formation of YAP/RUNX2 complex and BARX1 transcription. Cell Prolif 2019; 52: e12522.

30) Berlato C, Chan KV, Price AM, Canosa M, Scibetta AG, Hurst HC. Alternative TFAP2A isoforms have distinct activities in breast cancer. Breast Cancer Res 2011; 13: R23.

31) Jonckheere N, Fauquette V, Stechly L, Saint-Laurent N, Aubert S, Susini C, Huet G, Porchet N, Van Seuningen I, Pigny P. Tumour growth and resistance to gemcitabine of pancreatic cancer cells are decreased by AP-2alpha overexpression. Br J Cancer 2009; 101: 637-644.

32) Schulte JH, Kirfel J, Lim S, Schramm A, Friedrichs N, Deubzer HE, Witt O, Eggert A, Buettner R. Transcription factor AP2alpha (TFAP2a) regulates differentiation and proliferation of neuroblastoma cells. Cancer Lett 2008; 271: 56-63.

33) Sun X, Ou Z, Chen R, Niu X, Chen D, Kang R, Tang D. Activation of the p62-Keap1-NRF2 pathway protects against ferroptosis in hepatocellular carcinoma cells. Hepatology 2016; 63: 173-184.

34) Luo M, Wu L, Zhang K, Wang H, Zhang T, Gutierrez L, O'Connell D, Zhang P, Li Y, Gao T, Ren W, Yang Y. miR-137 regulates ferroptosis by targeting glutamine transporter SLC1A5 in melanoma. Cell Death Differ 2018; 25: 1457-1472.

35) Li R, Jia Z, Zhu H. Regulation of Nrf2 signaling. React Oxyg Species (Apex) 2019; 8: 312-322.

36) Zhang M, Zhang C, Zhang L, Yang Q, Zhou S, Wen Q, Wang J. Nrf2 is a potential prognostic marker and promotes proliferation and invasion in human hepatocellular carcinoma. BMC Cancer 2015; 15: 531.

37) Ryoo IG, Choi BH, Ku SK, Kwak MK. High CD44 expression mediates p62-associated NFE2L2/NRF2 activation in breast cancer stem cell-like cells: implications for cancer stem cell resistance. Redox Biol 2018; 17: 246-258.

38) Shin D, Kim EH, Lee J, Roh JL. Nrf2 inhibition reverses resistance to GPX4 inhibitor-induced ferroptosis in head and neck cancer. Free Radic Biol Med 2018; 129: 454-462.